Cognitive Neurodynamics
https://doi.org/10.1007/s11571-024-10153-6

RESEARCH ARTICLE

STEADYNet: Spatiotemporal EEG analysis for dementia detection using convolutional neural network

Pramod H. Kachare[1,2] · Sandeep B. Sangle[2] · Digambar V. Puri[2] · Mousa Mohammed Khubrani[1] · Ibrahim Al-Shourbaji[1]

Received: 10 May 2024 / Revised: 21 June 2024 / Accepted: 10 July 2024

Abstract

Dementia is a neuro-degenerative disorder with a high death rate, mainly due to high human error, time, and cost of the current clinical diagnostic techniques. The existing dementia detection methods using hand-crafted electroencephalogram (EEG) signal features are unreliable. A convolution neural network using spatiotemporal EEG signals (STEADYNet) is presented to improve the dementia detection. The STEADYNet uses a multichannel temporal EEG signal as input. The network is grouped into feature extraction and classification components. The feature extraction comprises two convolution layers to generate complex features, a max-pooling layer to reduce the EEG signal's spatiotemporal redundancy, and a dropout layer to improve the network's generalization. The classification processes the feature extraction output nonlinearly using two fully-connected layers to generate salient features and a softmax layer to generate disease probabilities. Two publicly available multiclass datasets of dementia are used for evaluation. The STEADYNet outperforms existing automatic dementia detection methods with accuracies of 99.29%, 99.65%, and 92.25% for Alzheimer's disease, mild cognitive impairment, and frontotemporal dementia, respectively. The STEADYNet has a low inference time and floating point operations, suitable for real-time applications. It may aid neurologists in efficient detection and treatment. A Python implementation of the STEADYNet is available at https://github.com/SandeepSangle12/STEADYNet.git

Keywords Alzheimer's disease · Convolution neural network · Electroencephalogram · Frontotemporal dementia

Introduction

Dementia manifests as symptoms resulting from the impaired function of specific brain cell groups, impacting desires, reactions, and movement (Breijyeh and Karaman 2020). This neurodegenerative condition progressively damages neural cells in the human brain. The prevalence of Alzheimer's disease (AD) or dementia rises with increasing age, from 2% in the age group of 60–65 to 25–35% in 85 and above. When dementia emerges before 65, it's termed early-onset; after 65, it's classified as late-onset (Siuly et al. 2024). The condition can stem from various causes, reversible or otherwise. Notably, Mild cognitive impairment (MCI), frontotemporal dementia (FTD), and AD are the initial culprits behind early-onset dementia. AD disrupts brain neurons and axons, impacting cognitive impairments (Miltiadous et al. 2021). FTD involves focal degeneration in the temporal and frontal lobes, accompanied by islet atrophy. The FTD was first described in 1892,

✉ Ibrahim Al-Shourbaji
alshourbajiibrahim@gmail.com

Pramod H. Kachare
kachare.pramod1991@gmail.com

Sandeep B. Sangle
sandeepsangle12@gmail.com

Digambar V. Puri
digspuri@gmail.com

Mousa Mohammed Khubrani
mmkhubrani@jazanu.edu.sa

[1] Jazan University College of Engineering, Jazan, Saudi Arabia

[2] Department of Computer Science & Engineering, Ramrao Adik Institute of Technology, Navi Mumbai, India

Published online: 19 July 2024

delineating its symptoms like frontal lobe atrophy and aphasia. Previous efforts to classify FTD and AD based on cognitive functions such as concentration, executive function, or memory have yielded inconsistent or conflicting results (Miltiadous et al. 2023).

Misdiagnoses between MCI, AD, and FTD underscore the urgent need for more effective differentiation methods. The parietal neocortex, posterior temporal, and hippocampus areas are mainly affected by AD. On the other hand, FTD targets the frontal and temporal lobes of the human brain. Clinically, AD is characterized by neurofibrillary tangles and senile plaques affecting motor areas (visual and memory effect), whereas FTD presents with personality and behavioral changes. The MCI has shown no clinical evidence of changes in the neurons (Atri 2019).

Neuro-physiologists extensively employed neuro-imaging techniques and Electroencephalogram (EEG) to improve the diagnostic accuracy of AD and FTD (Modir et al. 2023; Kılıç and Aydın 2022). The techniques using magnetic resonance images, single-photons emission tomography utilizing 99mTc-HMPAO, and positrons emission tomography employing 18 FDG have significantly enhanced the diagnosis of AD and FTD (Cagnin et al. 2024). However, some diagnoses occur after significant neuro-degeneration is evident, highlighting the importance of accurately predicting the onset of dementia (Kachare et al. 2024). Early recognition and intervention are crucial for effective treatment planning and developing new therapies to manage the disease's progression (Cai et al. 2024; Aydın 2022).

Clinical AD diagnosis using various blood, neurological, and psychological tests is subject to a neurologist's expertise (Ghorbanian et al. 2015). Neuroimaging techniques for detecting AD are radiogenic, expensive, and time-inefficient (Jiao et al. 2023). An EEG-based safer approach investigates brain abnormalities in AD patients for non-invasive and cost-effective automatic AD detection (Yuan et al. 2018). Normal controlled (NC) subject's EEG has more complexity, synchrony, and less slowing than AS patient's EEG (Giudice et al. 2019).

Several models for detecting AD and FTD from NC subjects by extracting EEG-based features are reported in literature (Dauwels et al. 2010). The recently reported methods are presented in Table 1. The literature suggests that most AD, FTD, and MCI detection methods have struggled to balance efficiency and accuracy satisfactorily. Many of these approaches rely on similar features such as coherence, complexity features, power spectrogram, and functional connectivity features coupled with machine learning models. Moreover, the datasets used in these studies have tended to be small, resulting in performances that are deemed comparable and ultimately not promising. Furthermore, there needs to be more research exploring the collective influence of FTD, AD, and MCI as a potential bio-feature for AD identification within the existing literature.

Nour et al. (2024) ensembled five different 2-D convolution neural network (2D-CNN) models to investigate the performance of AD detection. They achieved 97.90% average classification accuracy. However, CNN's hyperparameters are kept un-optimized to obtain the best performance. Ravikanti and Saravanan (2023) introduced an optimized transformer long-short term memory (LSTM) for AD EEG detection. They applied a third level to decompose EEG signals from lifting wavelets into multiple subbands. To obtain both temporal and spatial features from the decomposed signal, a fusion of recurrent neural network (RNN) and CNN. They obtained improvement in the accuracy by 2% than CNN. Nonetheless, this model fails to include many subjects for AD detection. Recently, Miltiadous et al. (2023) investigated spectral coherence connectivity and band power from FTD, AD, and NC. A dual input CNN encoder (DICE-Net) was trained with these features and obtained the performance of binary classification (FTD vs. AD, AD vs. NC, and FTD vs. NC). However, it was not generalized. In Siuly et al. (2024), power spectral density (PSD)-based biomarkers from band rhythms of various channels and LSTM with classification parameters adapted for the best accuracy of 97%. The UNet and similar CNNs, motivated by the success in computer vision reported in the literature, increased memory requirements and computational complexity during training and testing. The larger number of floating-point operations resulted in higher inference time. Hence, a lightweight CNN with low inference time and comparative AD detection performance is needed.

To overcome these issues, the present study introduces a novel low-complex convolutional neural network (STEADYNet) for automatically identifying three distinct types of EEG signals: MCI, AD, and FTD, aiming to enhance detection and classification performance. The critical innovation comes from our combined effort to reduce computations with high accuracy. The computation complexity depends on total trainable parameters with the floating point methods within the CNN model. Hence, our primary objective is to minimize the trainable parameters by developing an architecture that includes the minimum number of weighted layers, thereby reducing the computational burden and enhancing the overall efficiency of the proposed model.

The main contributions of the present work are:

- Introducing a novel lightweight CNN architecture, STEADYNet, specifically developed for EEG-based automatic detection of AD, FTD, and MCI.

Table 1 Earlier reported methods for AD, MCI, and FTD detection

References	Year	Features	Channels	Subjects	Classifier	Accuracy (%)	Sensitivity (%)	Specificity (%)
Calub et al. (2023)	2023	non-linear Uni-variate feature with PCA	21	AD:31, MCI:20, NC:35	KNN	97.64	95.40	98.81
Fouad and Labib (2023)	2023	Contrast, & wavelet statistical features	19	AD:59, MCI:7, NC:102	ResNet	97.82	97.83	98.26
Chang and Chang (2023)	2023	Ratio of powers from temporal and frontal lobes	19	NC:29, FTD:29	Logistic regression	76.92	69.60	86.20
Miltiadous et al. (2023)	2023	PSD of subbands + LOSO	19	AD:36 FTD:23 NC:29	RF MLP	AD/NC:- 77.01 FTD/NC:- 73.12	78.32 63.00	80.94 78.63
Ding et al. (2022)	2022	Spectral, & complexity features	5	NC:113, MCI:116, AD:72	SVM	AD/ MCI:- 69.10 AD/NC:- 72.42 MCI/NC:- 59.90	69.76 65.27 92.82	62.41 76.98 57.13
Ho et al. (2021)	2022	ER-SP feature	19	NC:23, AD:40	CNN-LSTM	75.95	77.23	69.40
Geng et al. (2022)	2022	Spectral, complexity features	16	NC:20, AD:20	SVM GRU	90.51 93.46	93.33 93.33	93.60 93.60
Chedid et al. (2022)	2022	Average PSD of periodogram	32	NC:23, AD:20	LR	81.11	75.00	79.33
Alvi et al. (2022)	2022	EEG Spectrogram	19	NC:11, AD:16	LSTM	96.91	97.95	96.16
Cejnek et al. (2021)	2021	Adaptive filtered feature	21	AD:59, MCI:7, NC:102	CV	90.73	92.03	85.71
Safi and Safi (2021)	2021	Linear, PSD & EMD based features	20	AD1:59, AD2:7, NC:102	ANN	93.74	94.91	98.56

GRU: Gated Recurrent Unit; KNN: k-nearest neighbor; PCA: Principle component analysis; ANN: Artificial neural network; LOSO: Leave one subject out; EMD: Empirical mode decomposition, SVM: Support vector machine; RF: Random forest; CV: Cross-validation

- Demonstrating the utilization of intrinsic redundancy within EEG signals to derive complex spatiotemporal features that enhance the discriminative capabilities of the model.
- Proposing strategies to reduce the computational complexity by optimizing inference time and floating-point operations.
- Investigating the STEADYNet layers to visualize the discriminative capabilities between classes in EEG dementia signals.
- Validating the present method performance by comparing with deep learning methods.

The remaining paper is structured as follows: The method and material of the present framework are described in "Methodology" section. Experimental results obtained from the present work are discussed in "Results and discussion" section. The conclusions of the present work are provided in "Conclusion" section.

Methodology

The CNN model recognizes intricate patterns in EEG signals and enhances the reliability and precision of dementia detection. Figure 1 shows the schematic of the proposed low-complexity CNN architecture for the dementia detection system. The section explains the dataset, pre-

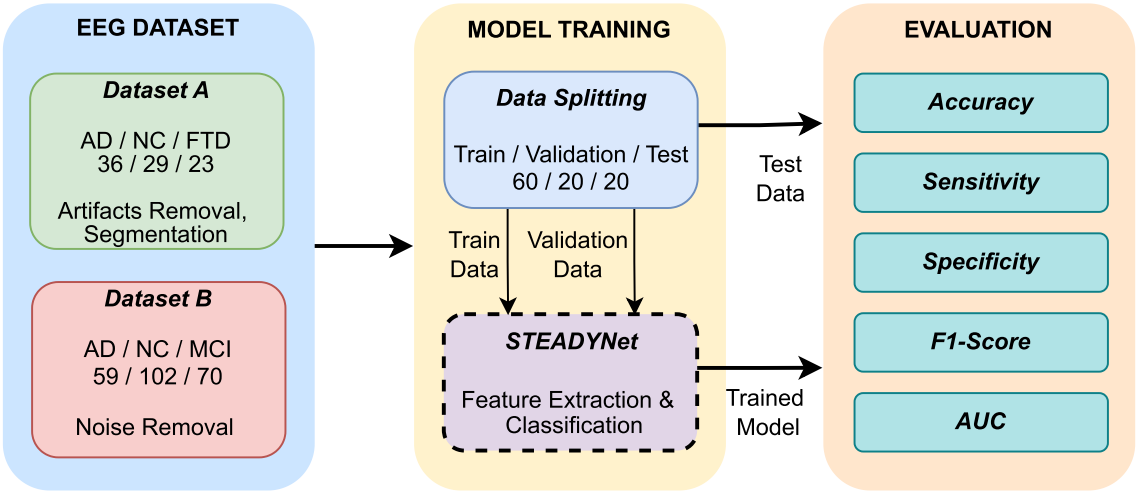

Fig. 1 Schematic flow of proposed work

processing techniques, the proposed architecture, and evaluation measures.

EEG Dataset

Here, open-source EEG datasets have been used to validate the presented work. The data description is given below.

Dataset-A (FTD, AD, and NC EEG data)

The open-access FTD, AD, and NC EEG dataset from OpenNeuro has been used in the present study (Miltiadous et al. 2023). Neurology experts recorded the EEG signals of different groups in the General Hospital of Thessaloniki. The subject details for all three classes are presented in Table 2. The EEG signals were recorded in closed-eye resting state conditions from 19 electrodes. The recording of each EEG signal lasted 13.5 min for AD, 12 min for FTD, and 13.8 min for NC. The 500 Hz sampling frequency and the resolution was $10\mu V/mm$ were utilized to sample the signals. All EEG signals were recorded according to NINCDS-ADRDA.

Table 3 EEG dataset details used in this work

Parameters	AD Patients	MCI Patients	NC subjects
No. of subjects	59	70	102
Age (years)	70.5 ± 4.9	67 ± 7.6	72 ± 5.3
Male/female	29/31	30/40	43/59
Sampling frequency (fs)	256 Hz	256 Hz	256 Hz
Number of channels	19	19	19
Duration (seconds)	7.8	7.8	7.8
Samples per signal	1000	1000	1000

Recordings were filtered with a bandpass filter with frequencies ranging from 0.5 to 45 Hz. Afterward, the ASR (artifact subspace reconstruction) method was employed to remove the transients or large-magnitude artifacts. The ICA (RunICA algorithm) command in EEGLAB was performed to remove the muscle, jaw, and eye-blink artifacts by considering 19 electrodes as 19 independent components.

Table 2 The AD, FTD, and NC EEG dataset details

Parameters	AD	FTD	NC
MMSE	17.75 ± 4.5	22.17 ± 8.22	30
Age (years)	66.40 ± 7.9	63.6 ± 8.20	67.9 ± 5.4
Subjects (male/female)	36 (13/23)	23 (14/9)	29 (11/18)
Disease duration (months)	25 ± 9.88	23 ± 9.35	–
Number of channels	19	19	19
Sampling frequency (Samples/second)	500	500	500

Dataset-B (AD, MCI, and NC EEG data)

This dataset has EEG recordings from AD, NC, and MCI subjects. The signals were recorded with closed eyes and the rest position of the subjects. Details of dataset-II are available in Cejnek et al. (2021). This dataset was sanctioned by the Ethics Committee of Hospital Hradec Kralove (HHK)) with Charles University in Prague, Czech Republic (CUPCR). The noise is eliminated by using EEGLAB. The subject details of the used dataset are presented in Table 3.

Low-complexity CNN architecture

A new CNN architecture capable of detecting AD, MCI, and FTD is presented, ensuring faster predictions, reduced memory usage, and shorter training times (Radhika et al. 2023). The weighted layers optimize the CNN architecture's trainable parameters and minimize the number of layers. The proposed low-complex CNN architecture for EEG dementia detection, called STEADYNet by the author, is characterized by its low complexity, minimal floating-point operations, and short inference time.

There are two main components for CNN architecture: (i) the feature extractor, which extends from CNN input layers to the flattened layer, and (ii) the classifier, extending from the flattened layer to the output layer (Al-Shourbaji et al. 2023). Figure 2 shows the proposed STEADYNet architectures for multi-class datasets 1 (AD, NC, and MCI) and 2 (AD, NC, and FTD).

The feature extraction component STEADYNet processes multi-channel temporal EEG data and extracts features from them. The high-dimensional feature is generated using two convolution layers and a max-pooling layer. The EEG data includes 19 electrodes, represented by 1024 voltage values over four seconds, as previously described in Sect. 2.1. Therefore, the input data for STEADYNet has a shape, becoming (19, 1024).

In the 2D convolution layer, kernel weights capture highly informative features and patterns within features specific to a particular task. The feature extraction layer of STEADYNet generates coarse features by fusing the spatiotemporal contents from the EEG data. The equation (1) extracts features from convolution layers.

$$conv[n] = Y(n,s) = \sigma\left(\sum_{k_1=0}^{2}\sum_{k_2=0}^{2} X(n+k_1, s+k_2)\cdot D_F(k_1,k_2) + b\right) \tag{1}$$

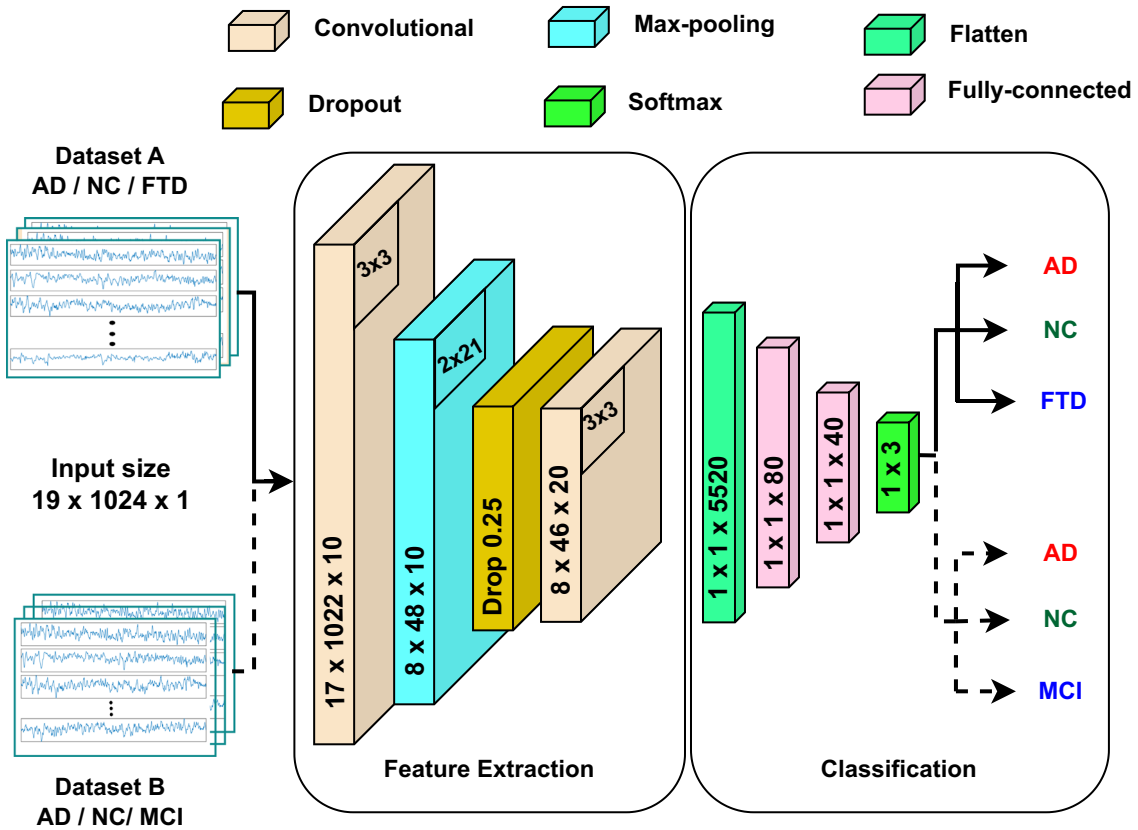

Fig. 2 Proposed STEADYNet model for Dataset A and B

Table 4 An architectural details of STEADYNet model

Layer type	Shape	Output Shape	Parameters
Input	N, S, 1	(19,1024,1)	
Conv2D	$(N-F+1),(S-F+1),D_F$	(17, 1022, 10)	100
MaxPool2D	$\left\lfloor\frac{N-F}{r_1}\right\rfloor,\left\lfloor\frac{S-F}{r_2}\right\rfloor,D_F$	(8, 48, 10)	0
Dropout			
Conv-2D	$\left(\left\lfloor\frac{N-F}{r_1}\right\rfloor-k\right),\left(\left\lfloor\frac{S-F}{r_2}\right\rfloor-k\right),2D_F$	(6, 46, 20)	1820
Flatten	$\left(\left\lfloor\frac{N-F}{r_1}\right\rfloor-k\right)\left(\left\lfloor\frac{S-F}{r_2}\right\rfloor-k\right)2D_F$	(2760)	0
FC	D_c	(80)	441,680
FC	$\frac{D_c}{2}$	(40)	3240
Softmax	C	(3)	123
Total			4,46,963

Here, $Y(n, s)$ represents the output at position (n, s) in the feature map. $X(n+k_1, s+k_2)$ is the input data at position $(n+k_1, s+k_2)$. n represents number of EEG channels and s represents EEG time samples. $D_F(k_1, k_2)$ denotes the convolution kernel's and k_1 and k_2 represent the dimensions of the convolution kernel. i.e. (3×3). b is the bias term.

The $\sigma(.)$ is a function that represents the activation function; here, a Rectified Linear Unit (ReLU) is employed element-wise to introduce non-linearity. In the first convolution layer, stride and padding are set to the default values. L2 regularization 0.1 was used to reduce the overfitting problem. It uses ten feature extracted Kernels representing D_F in Table 4, with the input data and output a feature map of shape (17, 1022, 10).

The EEG signals low-frequency components are most important for their ability to provide insight into the intrinsic redundancy within the temporal sequence. These low-frequency components can indicate patterns and correlations that may not be visible in higher-frequency signals. In the max-pooling layer, A 2×21 max-pooling kernel selected the maximum values from the input feature map 17×1022. A max-pooling layer captures the spatiotemporal redundancy in the EEG data. They selected significant patterns and extended the scope of successive convolutions (Al-Shourbaji et al. 2023; Aslam et al. 2024). The output of max-pooling layer $g_{max}(.)$ is computed as:

$$g_{max}(a,b) = max[S(h,v), S(h+r_1,v), S(h,v+r_2), S(h+r_1,v+r_2)] \quad (2)$$

Here, h and v are horizontal and vertical indices of input of the max-pooling layer. Where the maximum value is selected from a set of values within the specified region of the input, determined by the dimensions r_1 and r_2 of the max-pooling kernel, the asymmetric kernel size in the max-pooling layer can capture higher temporal redundancy and extract the most essential features for further processing. After max-pooling, the feature map shape is (8, 48, 20). A 0.25% dropout layer is added to resolve the overfitting issue.

A second 2D convolution layer having 20 kernels, i.e. $2D_F$ of 3×3 size, is added to generate more complex spatiotemporal features, and L2 regularization is 0.1 to overcome the overfitting problem with an output shape of (5, 58, 10). A flatten layer rearranges the spatiotemporal feature map as a feature vector of 2760 dimensions, a product of all dimensions of the feature maps. The layer dimension calculations are shown in Table 4.

The classifier component processes the output of the feature extractor. It comprises two fully-connected layers (FC) to select the most important features while achieving a nonlinear transformation of the feature vector. The successive first and second FCs used 80 and 40 neurons to exponentially reduce the computational complexity (Al-Shourbaji et al. 2023). Lastly, the softmax layer generates disease probabilities. These can be used to understand the model's confidence, reliability, and interpretability.

The network weights are iteratively updated using the Adam optimizer. It combines the root mean square propagation (RMSP) and stochastic gradient descent (SGD) to simplify each weight's learning rate. For t^{th} example, $y_p(t,k)$ is the k^{th} probability with $\sum_k y_p(t,k) = 1, \forall t$. A cross-entropy loss ($L$) is used, and it can be computed as:

$$L = -\sum_{t-1}^{N_t}\sum_{k-1}^{N_c} y(t,k) \times \log y_p(t,k) \quad (3)$$

where N_t is total training examples and N_c is total classes. The shape, kernel, and parameter details of the proposed STEADYNet are provided in Table 4.

Table 5 Performance evaluation of Dataset A (AD vs. FTD vs. NC) and Dataset B (AD vs. MCI vs. NC) using STEADYNet model

Model	Dataset	CA (%)	SE (%)	SP (%)	F1 (%)	AUC (%)
Dataset-A	Training	94.66	94.43	97.51	94.71	96.13
	Validation	85.17	85.09	92.87	85.37	88.75
	Testing	84.59	84.58	82.56	84.63	88.02
Dataset-B	Training	98.28	98.25	99.14	98.27	99.08
	Validation	96.85	96.79	98.39	96.79	97.83
	Testing	97.59	94.11	95.52	97.54	98.24

Computation complexity

The size and count of channels influence the parameter quantity in convolutional systems. The parameters are available in fully-connected and convolution layers. The flatten layer only transforms the shape of the feature map and does not introduce any additional parameters. Training parameters for a given layer are computed using the equation (4),

$$\text{Trainable parameters} = (((k_1 \times k_2) \times (D_F - 1)) + 1)D_F \tag{4}$$

$(D_F - 1)$ indicates the number of filters used for feature extraction in the previous layer, and D_F refers to the number of filters used for feature extraction in that layer. As per the above equations, trainable parameters of The first two convolution layers contribute $((3 \times 3 \times 1) + 1)10 = 100$ and $((3 \times 3 \times 10) + 1)20 = 1820$ trainable parameters, respectively.

Kernel size has not come into action to calculate trainable parameters of FC layers because the kernel is unused. The trainable parameters of the first and second dense layers are $(5520 + 1)50 = 4,41,680$ and $((80 + 1)40 = 3240$. These layers account for approximately 98.56% of the STEADYNet trainable parameters. Hence, the STEADYNet is carefully designed to restrict the number of convolution and FC layers. The max-pooling layer does not have trainable parameters, but the asymmetric kernel reduced the size of the feature map input to the second convolution layer. Hence, it reduces the total trainable parameters. The softmax layer has only 123 trainable parameters. Table 4 outlines the discrepancy in the overall count of trainable parameters between the proposed architectures and those already reported. The number of trainable parameters in STEADYNet architecture is 4,46,963. Figure 2 shows the behavior of proposed STEADYNet architectures towards overall trainable parameters, respectively.

Mega Floating Point Operations per Second (MFLOPS) (Miltiadous et al. 2023), the total number of floating point multiplications and additions per second. FLOPs are important for evaluating neural network models' efficiency and computational requirements. Here, the FLOPs calculations for different STEADYNet layers are shown. The convolution layer's FLOP value is calculated using equation (5),

$$FLOP_{conv} = 2 \times (Y(n, s) \times D_F \times (k_1 \times k_2)) \tag{5}$$

$Y(n, s)$ and (k_1, k_2) are the Output of convolutional layers and kernel window shape. As per the equations (5), the FLOP value of the first and second convolutional layer is $2 \times (17 \times 1022 \times 10 \times 3 \times 3)) = 31,27,320$ and $2 \times (6 \times 46 \times 20 \times 3 \times 3)) = 99,360$. FLOPs of Pooling layers are calculated using equation (6) and become 46080.

$$FLOP_{pool} = \frac{a}{s} \times d \times \frac{b}{s} \tag{6}$$

Here, b and a are vertical and horizontal indices, and s is stride.

The FLOP for FC layers is calculated using equation (7). For the First and second FC layers, FLOP values are $(2 \times (6 \times 46 \times 20 \times 80) = 8,83,200)$ and $(2 \times (40 \times 80) = 6,400)$.

$$FLOP_{FC} = 2 \times \text{Input size} \times \text{Output size} \tag{7}$$

The STEADYNet with an 5.353M MFLOPS and 0.35 sec inference time is suitable for real-time applications.

Table 6 Class pair-wise performance evaluation of Dataset -A and Dataset-B using STEADYNet model

Model	Dataset	CA (%)	SE (%)	SP (%)	F1 (%)	AUC (%)
Dataset-A	AD versus FTD	89.40	85.32	92.05	87.71	90.13
	AD versus NC	88.00	82.59	91.88	88.00	87.18
	FTD versus NC	92.25	87.97	94.04	87.48	90.35
Dataset-B	AD versus MCI	97.72	99.52	90.62	98.55	92.23
	AD versus NC	99.29	99.52	98.71	99.52	96.11
	MCI versus NC	99.65	97.97	100	98.98	98.98

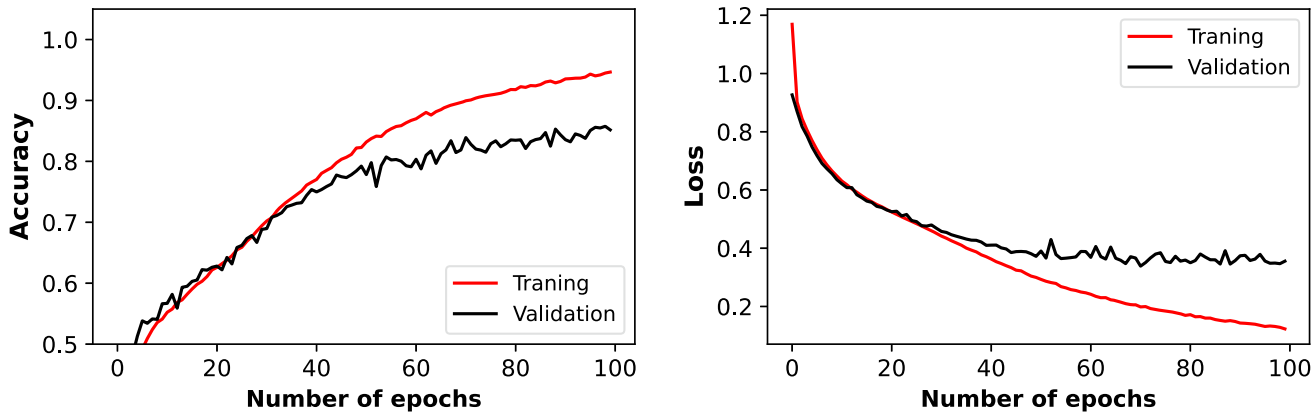

Fig. 3 STEADYNet accuracy and loss using Dataset A

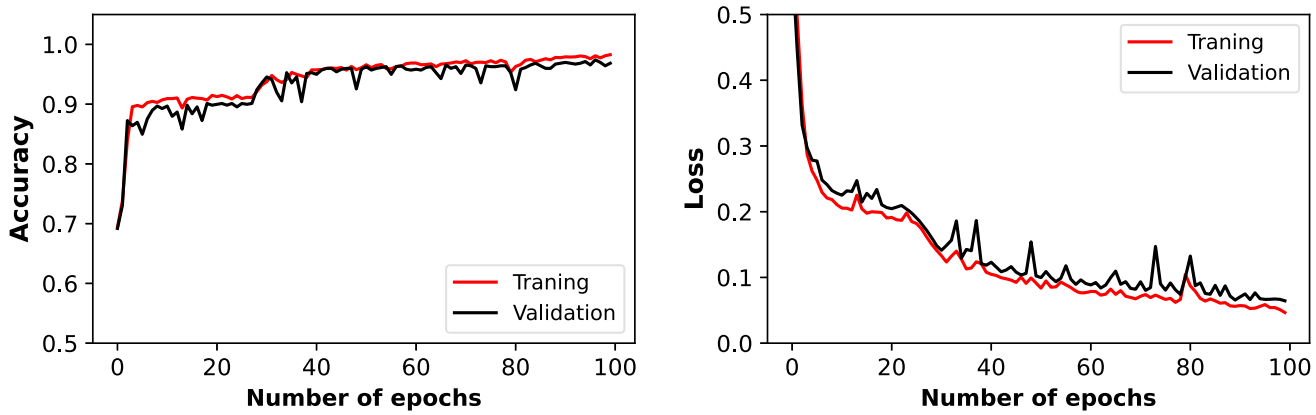

Fig. 4 STEADYNet accuracy and loss using Dataset B

Evaluation metrics

The detection ability of models is evaluated using classification accuracy (CA), specificity (SP), sensitivity (SE), F1-score (F1), and area under the receiver operating curve (AUC). These parameters are calculated as (Tharwat 2021):

$$CA = \frac{S_{pp} + S_{nn}}{S_{pp} + S_{pn} + S_{pn} + S_{nn}} \times 100 \tag{8}$$

$$SP = \frac{S_{nn}}{S_{nn} + S_{np}} \times 100 \tag{9}$$

$$SE = \frac{S_{pp}}{S_{pp} + S_{pn}} \times 100 \tag{10}$$

$$F1 = \frac{2 \times S_{pp}}{2 \times S_{pp} + S_{np} + 2S_{pn}} \times 100 \tag{11}$$

Here, S_{ij} is the i^{th} subject class that is predicted to be in j^{th} class, where $i,j \in \{p,n\}$ indicates dementia class.

Results and discussion

The experiments used a machine with Nvidia (P100) GPU, 16 GB of RAM, a 1.32 GHz Processor, the Linux Operating system, and Python-based TensorFlow libraries. Here, The EEG signals are segmented into 1024 samples to maintain the identical input shape to CNN layers. After segmentation, 34,052 total samples are used for dataset A, and 4261 samples are used for dataset B. The EEG recordings provided as input are grouped into three subsets: training, validation, and testing. These subsets are allocated 60%

Adam, an adaptive optimization algorithm, adjusts the learning rates of each parameter individually, potentially helping the model converge faster and avoid over-fitting. The Adam optimizer is used with an initial learning rate of 0.0001 and 0.001 for Dataset A and B, respectively. The two hyper-parameters that affect the class detection performance are batch size and epoch. The batch size is searched linearly from 20 to 200 in step 5, and the number of epochs is searched linearly from 10 to 150 in step 10.

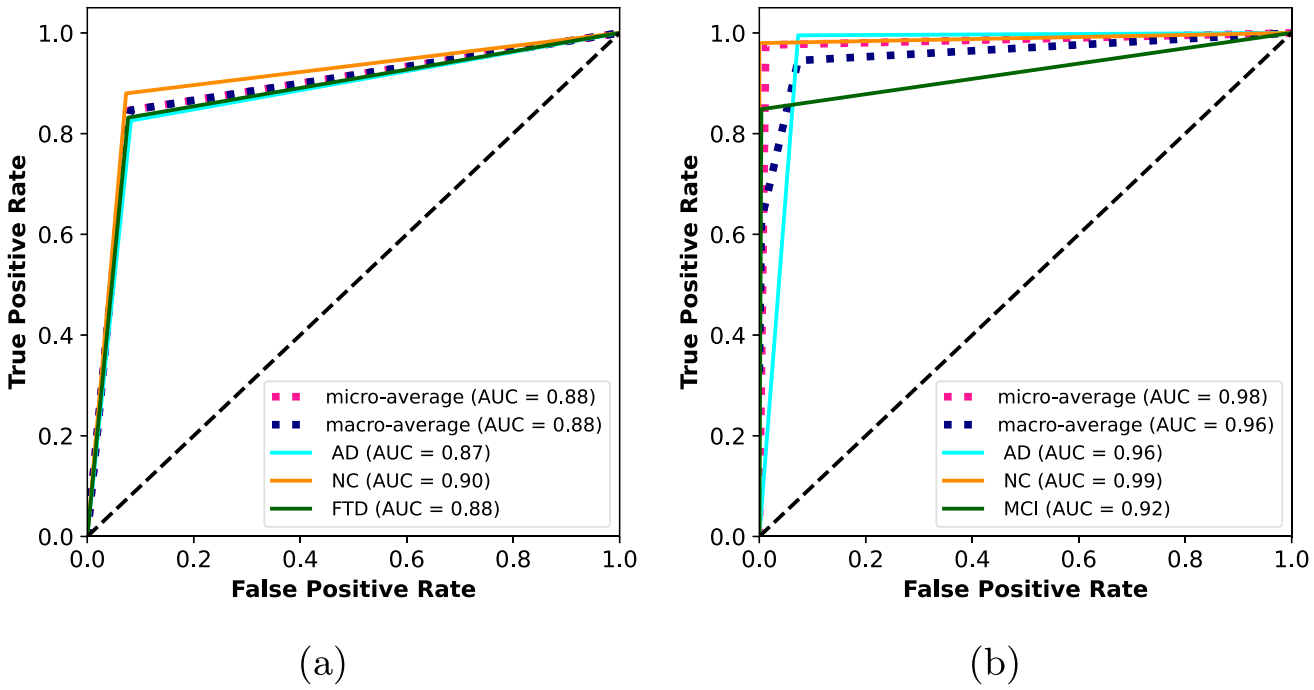

Fig. 5 ROC curve of each class using proposed STEADYNet on (a) dataset A and (b) dataset B

The best performance is obtained for batch size 80 and the maximum number of epochs 100.

The performance metrics of the proposed STEADYNet model compared with Dataset A and B using CA, F1-score, SE, SP, and AUC are presented in Table 5. For Dataset A, during the training phase, the model achieves a high accuracy of 94.66%. This high accuracy indicates that the model has successfully learned and generalized patterns from the training data. In the testing phase, the model maintains an accuracy of 84.59%, a sensitivity of 84.58%, and a specificity of 82.56%, indicating its ability to capture all three class instances. F1 score 84.63% metrics give a balance between precision and recall during testing. These metrics suggest the model performs well on unseen data, showing its robustness and ability to accurately classify instances from different classes. The high accuracy, sensitivity, and specificity values indicate that the model effectively identifies instances from all three classes.

For the AD versus FTD classification using Dataset A presented in Table 6, the model performs well with an accuracy of 89.40% and F1-score of 87.71%. The high accuracy and F1 score indicate that the model effectively distinguishes between the two classes with a low misclassification rate. The AUC value of 90.13% indicates good discriminative ability for this class pair. In the AD versus NC class, the model achieves an accuracy of 88.00%. For the FTD versus NC comparison, the model achieves an accuracy of 92.25%. The sensitivity 87.97% and specificity 94.04% metrics suggest that the model effectively captures FTD cases.

For Dataset B, In the training and validation phase, the STEADYNet model demonstrates exceptional performance, achieving high accuracy of 98.28% and 96.85%, respectively. In the testing phase, the model exhibits robust overall accuracy of 97.59% with an F1-score of 97.54%. The sensitivity 94.11 and specificity 95.52% are high, which emphasizes the model's proficiency in correctly classifying EEG signals. The MCC of 94.53% and Kappa coefficient of 94.45 further reported the overall strong performance of the STEADYNet model on Dataset-1 during the testing phase.

For the AD versus MCI class pair in Dataset-B, the STEADYNet model achieves an accuracy of 97.72%. The model demonstrates a strong sensitivity of 99.52%, specificity of 90.62%, and F1 score of 98.55%, indicating its effectiveness in correctly identifying cases of AD and MCI. The AUC value of 92.23% further supports the model's discriminative ability for this class pair. Similarly, in the AD versus NC class pair, the model achieved an accuracy of 99.29%, with high sensitivity 99.52%, specificity 98.71%, and F1 score 99.52%. In the MCI versus NC class pair, the STEADYNet model achieves perfect performance metrics, with 99.65% for all performance parameters.

The convergence analysis STEADYNet has been performed on both datasets. From the convergence analysis, the stability of learning patterns can be learned over many epochs. Figure 3 and 4 show the model's convergence over

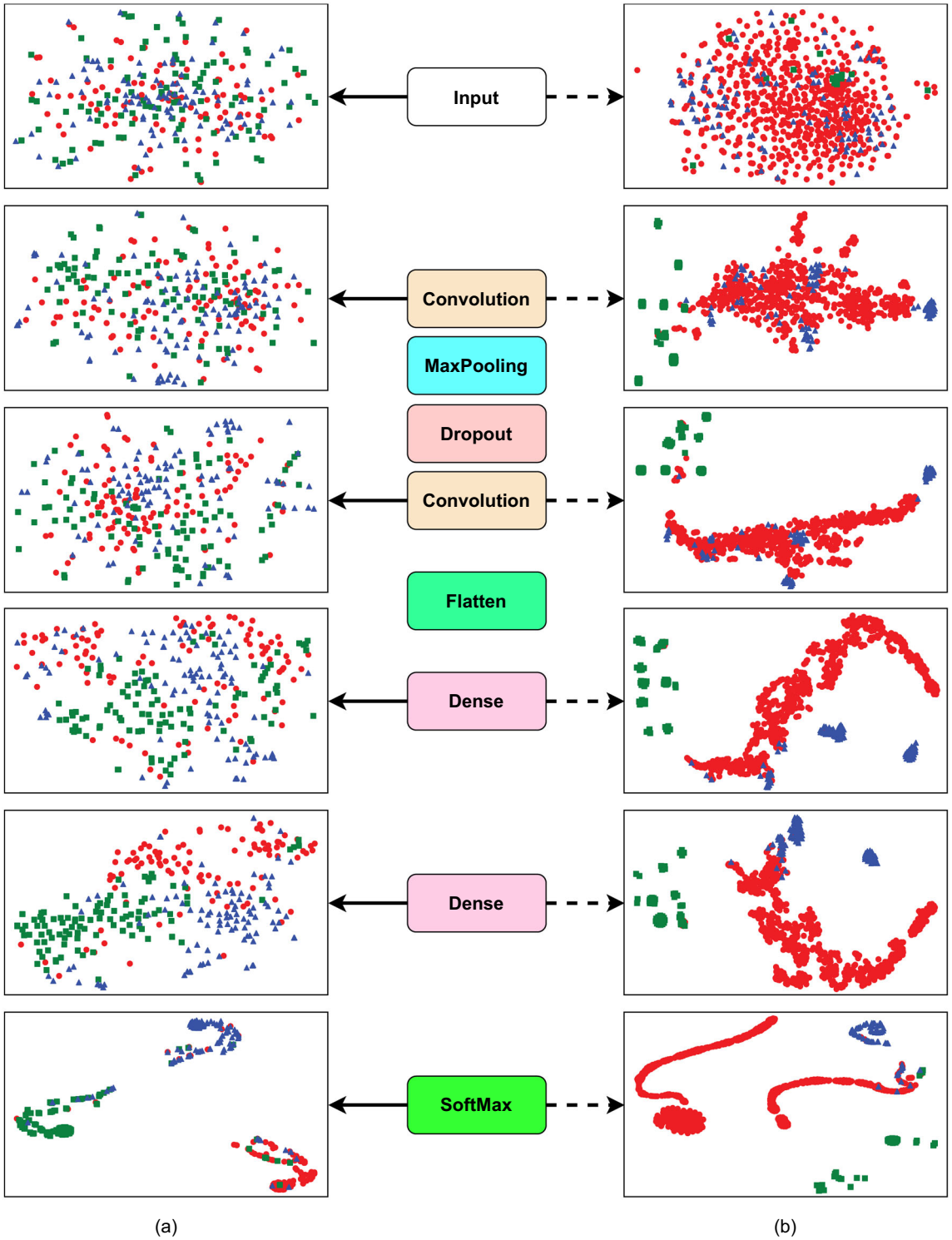

Fig. 6 A t-SNE visualization of STEADYNet using datasets A and B

time using accuracy and loss plots. These plots indicate the enhancement of the model performance towards an optimal solution.

In Fig. 5 the regions of convergence (ROC) show the performance of the STEADYNet model on Datasets A and B, respectively. Notably, the NC class consistently gives the highest AUC values for both datasets. Specifically, for the AD class, AUC values reach 87% and 96%

Table 7 Comparative analysis with earlier methods using dataset A

Ref	Method	CA (%)	SE (%)	SP (%)
Miltiadous et al. (2021)	Statistical, spectral features with RF	AD versus NC: 98.10	98.60	99.00
		FTD versus NC: 98.00	98.00	98.00
		AD versus FTD: 97.70	97.80	97.50
Zheng et al. (2023)	Spectral, complexity and synchronization features with RF	AD versus NC: 95.86	96.41	97.40
Miltiadous et al. (2023)	Band power, Spectral coherence connectivity with CNN	AD versus NC: 83.28	78.81	87.94
		FTD versus NC: 74.96	60.62	78.63
Miltiadous et al. (2023)	EEG subbands PSD + LOSO ML models with RF	AD versus NC: 77.01	78.32	80.94
Chang and Chang (2023)	Ratio of powers from temporal and frontal lobes with LR	AD versus NC: 76.92	69.60	86.20
Chen et al. (2023)	Dual branch feature fusion network with visual transformer with CNN	AD versus NC: 84.56	85.15	88.19
		FTD versus NC: 81.66	82.55	83.41
		AD versus FTD: 79.81	80.77	82.19
		AD versus FTD versus NC: 77.09	78.30	80.23
This work	STEADYNet	AD versus FTD: 89.40	85.35	92.05
		AD versus NC: 88.00	82.59	91.88
		FTD versus NC: 92.25	87.97	94.04
		AD versus FTD versus NC: 84.59	84.58	82.56

Layer visualization

The data distribution using STEADYNet is visualized in Fig. 6, with each class sample having different colors and markers. The t-distributed stochastic neighbor embedding (t-SNE), a dimensional reduction technique that maps high-dimensional data into a lower-dimensional space, approximates the data distribution is approximated using. The t-SNE-based STEADYNet visualization provides insights into the model and shows class separation. It helps to understand the clustering and separability of the data in the STEADYNet model.

Figure 6 represents the input layer of the STEADYNet network using Dataset A and B, respectively. It shows that the majority of EEG signals from all three classes share similar characteristics in terms of their spatial distribution. The high density at the center might indicate a typical pattern or feature present across different EEG signal types.

Figure 6, depicts the visualization of STEADYNet convolutional layers 1 and 2 using datasets A and B, respectively. These layers work as feature extraction tasks in the STEADYNet model. As features of EEG signals move from layer 1 to 3, changes in its distribution. It is indicated that STEADYNet extracts highly informative features and passes them to flatten and dense layers for classification. For Dataset A and Dataset B, the distance between each class distribution increases, indicating high performance in detecting EEG signals.

Comparison with existing models

A comparison of the STEADYNet and existing models using Dataset-A is presented in Table 7. Miltiadous et al. (2023) introduced a method for FTD detection based on spectral features and conducted binary classification, achieving a peak accuracy of 98.10% for distinguishing AD from NC with a limited dataset. However, when tested on a larger dataset, their approach yielded a significantly lower accuracy of 77.01%, indicating inconsistency and potential overfitting issues. Notably, their study did not extend to the 3-class classification scenario. In a subsequent study in 2023, the same authors (Miltiadous et al. 2023) explored a dual-input CNN incorporating spectral and connectivity-based features, achieving an accuracy of 83.28% for AD versus NC classification. Dataset-A used in this study is publicly available, prompting other researchers (Zheng et al. 2023) to investigate spectral, complexity, and synchronization features using random forest (RF) and LOSO cross-validation, resulting in an accuracy of 95.86% for AD versus NC classification. However, it's important to note that this method's performance was evaluated solely

Table 8 Comparative analysis with earlier methods using dataset B

Ref	Method	CA (%)	SE (%)	SP (%)
Calub et al. (2023)	Linear & non-linear Uni-variate features + PCA with KNN	AD versus NC: 95.64	95.40	98.81
Cejnek et al. (2021)	Adaptive filtering based novelty features with DT	AD versus NC: 90.29	89.51	90.73
Wang et al. (2023)	Topological features with CNN	AD versus NC: 96.26	–	–
Sadegh-Zadeh et al. (2023)	Variational encoder with PSD features and CNN	AD versus NC: 88.25	90.15	88.86
This work	STEADYNet	AD versus MCI:97.72	99.52	90.62
		AD versus NC: 99.29	99.52	98.71
		MCI versus NC: 99.65	97.97	100
		AD versus MCI versus NC: 97.59	94.11	95.52

with fixed RF parameters, indicating a need for hyperparameter tuning to ensure improved and consistent results. Chen et al. (2023) mentioned CNN-based approach with fused features from visual transformer for two and 3-class classification. The authors reached up to 84.56% accuracy for AD versus NC. The proposed model overcame these limitations and achieved the best performance compared to earlier reported methods in Table 7. The proposed STEADYNet model has 2% higher detection than existing models.

Similarly, Table 8 presents a comparative analysis between the current method and earlier approaches that utilized Dataset-B. Only a limited number of studies have utilized this open-access dataset. For instance, Cejnek et al. (2021) explored adaptive filtering novelty features extracted from AD, MCI, and NC EEG signals, employing decision trees for binary classification. However, they did not extend their analysis to a 3-class classification. Other researchers (Wang and Sun 2021; Calub et al. 2023; Sadegh-Zadeh et al. 2023) have employed deep learning models for classification, achieving the highest accuracy of 96.26% for AD versus NC (Wang and Sun 2021), albeit at the expense of high computational complexity and time. In contrast, the proposed model achieved a superior accuracy of 98.28% for AD versus NC. Furthermore, the binary and multiclass classification performance of the current method demonstrates a 3–5% improvement over earlier approaches.

Advantages of the proposed STEADYNet

The goal of the current investigation is to develop a robust and low-complexity CNN model for improving dementia detection using the raw EEG data. Some of the advantages of the proposed STEADYNet are:

- The STEADYNet analyses multichannel channels EEG signal to generate fairly interpretable spatiotemporal features.
- The STEADYnet architecture, focused on a low-complexity approach, facilitates small inference time even on low-resource devices.
- The generalized architecture of the STEADYNet can easily be adapted to build detection systems for other brain disorders.

Limitations and future directions

Although the STEADYNet outperformed the existing models, it has some limitations. Two freely available datasets are relatively restricted in terms of the subjects. Factors such as age, gender, and medications affect performance. For example, AD patients of lower ages may perform well using the proposed model due to less age-related issues in AD and FTD signals. Most of these concerns may be addressed based on data availability. Although CNNs effectively learn complex data patterns, they are sensitive to data variations, and their decision process interpretation is challenging.

Building on the foundations laid by this research, some directions for future work are:

- Integration with existing clinical diagnosis techniques may aid the decision-making of neurologists.
- Application in real-time detection system will improve healthcare experience by continuous patient monitoring.
- Expansion of the available data in terms of ethnicities, demographics, and disease stages may improve the model's generalizability.
- Interpretation and visualization of the decision-making process may improve the model's adoption by clinical experts.

In the future, we aim to make cost-effective tools accessible to everyone for healthcare monitoring, brain-computer interfaces, and other areas where real-time EEG analysis is required.

Conclusion

An efficient CNN-based dementia detection model using the spatiotemporal EEG signal as an input, STEADYNet, is presented. The STEADYNet has a feature extractor comprising convolution, max-pooling, and dropout layers to generate nonlinear spatiotemporal EEG features. A classifier comprising fully-connected and softmax layers processes these features to predict disease probabilities. A comparative analysis showed the highest performance of the proposed STEADYNet compared to other existing models using two freely available datasets for AD, MCI, and FTD. The generalization was investigated by visualizing the model. The lower complexity of the proposed model makes it a strong candidate for real-world healthcare applications.

Funding Not applicable.

Data availibility Data is available, and the link is provided in the abstract.

Declarations

Conflict of interest The authors declare no Conflict of interest regarding this paper.

Ethical approval This article contains no studies with human participants or animals performed by authors. No human or animal subjects are involved in this study.

References

Al-Shourbaji I, Kachare PH, Abualigah L, Abdelhag ME, Elnaim B, Anter AM, Gandomi AH (2023) A deep batch normalized convolution approach for improving COVID-19 detection from chest X-ray images. Pathogens. https://doi.org/10.3390/pathogens12010017

Alvi AM, Siuly S, Wang H (2022) A long short-term memory based framework for early detection of mild cognitive impairment from EEG signals. IEEE Trans Emerging Top Comput Intell. https://doi.org/10.1109/TETCI.2022.3186180

Aslam MS, Radhika T, Chandrasekar A, Zhu Q (2024) Improved event-triggered-based output tracking for a class of delayed networked t–s fuzzy systems. Int J Fuzzy Syst 1–14

Atri A (2019) The Alzheimer's disease clinical spectrum: diagnosis and management. Med Clin N Am 103(2):263–293. https://doi.org/10.1016/j.mcna.2018.10.009. (**Neurology for the Non-Neurologist**)

Aydın S (2022) Cross-validated adaboost classification of emotion regulation strategies identified by spectral coherence in resting-state. Neuroinformatics 20(3):627–639. https://doi.org/10.1007/s12021-021-09542-7

Breijyeh Z, Karaman R (2020) Comprehensive review on Alzheimer's disease: causes and treatment. Molecules. https://doi.org/10.3390/molecules25245789

Cagnin A, Pigato G, Pettenuzzo I, Zorzi G, Roiter B, Anglani MG, Bussé C, Mozzetta S, Gabelli C, Campi C, Cecchin D (2024) Data-driven analysis of regional brain metabolism in behavioral frontotemporal dementia and late-onset primary psychiatric diseases with frontal lobe syndrome: a pet/mri study. Neurobiol Aging. https://doi.org/10.1016/j.neurobiolaging.2024.01.015

Cai Y, Peng Z, He Q, Sun P (2024) Behavioral variant frontotemporal dementia associated with GRN and ErbB4 gene mutations: a case report and literature review. BMC Med Genom 17(1):43. https://doi.org/10.1186/s12920-024-01819-5

Calub Gabriel Ivan A, Elefante Erickson N, Galisanao, Jose Colin A, Iguid Sofia Lyn Beatrice G, Salise Jeremae C, Prado Seigfred V (2023) EEG-based classification of stages of Alzheimer's disease (AD) and mild cognitive impairment (MCI). In: 5th international conference on bio-engineering for smart technologies (BioSMART), pp 1–6. https://doi.org/10.1109/BioSMART58455.2023.10162117

Cejnek M, Vyšata O, Valis M, Bukovsky I (2021) Novelty detection-based approach for Alzheimer's disease and mild cognitive impairment diagnosis from EEG. Med Biol Eng Compu 59:1–10. https://doi.org/10.1007/s11517-021-02427-6

Chang J, Chang C (2023) Quantitative electroencephalography markers for an accurate diagnosis of frontotemporal dementia: a spectral power ratio approach. Medicina 59(12):2155. https://doi.org/10.3390/medicina59122155

Chedid N, Tabbal J, Kabbara A, Allouch S (2022) The development of an automated machine learning pipeline for the detection of Alzheimer's disease. Sci Rep 12:18137. https://doi.org/10.1038/s41598-022-22979-3

Chen Y, Wang H, Zhang D, Zhang L, Tao L (2023) Multi-feature fusion learning for Alzheimer's disease prediction using EEG signals in resting state. Front Neurosci 17

Dauwels J, Vialatte F, Musha T, Cichocki A (2010) A comparative study of synchrony measures for the early diagnosis of Alzheimer's disease based on EEG. Neuroimage 49(1):668–693. https://doi.org/10.1016/j.neuroimage.2009.06.056

Ding Y, Chu Y, Liu M, Ling Z, Wang S, Li X, Li Y (2022) Fully automated discrimination of Alzheimer's disease using resting-state Electroencephalography signals. Quant Imaging Med Surg 12:1063. https://doi.org/10.21037/qims-21-430

Fouad IA, Labib FE-ZM (2023) Identification of Alzheimer's disease from central lobe EEG signals utilizing machine learning and residual neural network. Biomed Signal Process Control 86:105266. https://doi.org/10.1016/j.bspc.2023.105266

Geng D, Wang C, Fu Z, Zhang Y, Yang K, An H (2022) Sleep EEG-based approach to detect mild cognitive impairment. Front Aging Neurosci. https://doi.org/10.3389/fnagi.2022.865558

Ghorbanian P, Devilbiss D, Hess T, Bernstein A, Simon A, Ashrafiuon H (2015) Exploration of EEG features of Alzheimer's disease using continuous wavelet transform. Med Biol Eng Comput. https://doi.org/10.1007/s11517-015-1298-3

Ho TKK, Jeon Y, Na E, Ullah Z, Kim BC, Lee KH, Song J-I, Gwak J (2021) DeepADNet: a CNN-LSTM model for the multi-class classification of Alzheimer's disease using multichannel EEG. Alzheimer's Dement 17:057573. https://doi.org/10.1002/alz.057573

Jiao B, Li R, Zhou H, Qing K, Liu H, Pan H, Lei Y, Fu W, Wang X, Xiao X (2023) Neural biomarker diagnosis and prediction to

mild cognitive impairment and Alzheimer's disease using EEG technology. Alzheimer's Res Ther 15(1):1–14. https://doi.org/10.1186/s13195-023-01181-1

Kachare P, Puri D, Sangle SB, Al-Shourbaji I, Jabbari A, Kirner R, Alameen A, Migdady H, Abualigah L (2024) LCADNet: a novel light CNN architecture for EEG-based Alzheimer disease detection. Phys Eng Sci Med. https://doi.org/10.1007/s13246-024-01425-w

Kılıç B, Aydın S (2022) Classification of contrasting discrete emotional states indicated by EEG based graph theoretical network measures. Neuroinformatics 20(4):863–877. https://doi.org/10.1007/s12021-022-09579-2

Lo Giudice P, Mammone N, Morabito F, Pizzimenti R, Ursino D, Virgili L (2019) Leveraging network analysis to support experts in their analyses of subjects with MCI and AD. Med Biol Eng Comput. https://doi.org/10.1007/s11517-019-02004-y

Miltiadous A, Tzimourta KD, Giannakeas N, Tsipouras MG, Afrantou T, Ioannidis P, Tzallas AT (2021) Alzheimer's disease and frontotemporal dementia: a robust classification method of EEG signals and a comparison of validation methods. Diagnostics. https://doi.org/10.3390/diagnostics11081437

Miltiadous A, Tzimourta KD, Afrantou T, Ioannidis P, Grigoriadis N, Tsalikakis DG, Angelidis P, Tsipouras MG, Glavas E, Giannakeas N, Tzallas AT (2023) A dataset of scalp EEG recordings of Alzheimer's disease, frontotemporal dementia and healthy subjects from routine EEG. Data. https://doi.org/10.3390/data8060095

Miltiadous A, Gionanidis E, Tzimourta KD, Giannakeas N, Tzallas AT (2023) Dice-net: a novel convolution-transformer architecture for Alzheimer detection in EEG signals. IEEE Access 11:71840–71858. https://doi.org/10.1109/ACCESS.2023.3294618

Modir A, Shamekhi S, Ghaderyan P (2023) A systematic review and methodological analysis of EEG-based biomarkers of Alzheimer's disease. Measurement 220:113274. https://doi.org/10.1016/j.measurement.2023.113274

Nour M, Senturk U, Polat K (2024) A novel hybrid model in the diagnosis and classification of Alzheimer's disease using EEG signals: deep ensemble learning (DEL) approach. Biomed Signal Process Control 89:105751. https://doi.org/10.1016/j.bspc.2023.105751

Radhika T, Chandrasekar A, Vijayakumar V, Zhu Q (2023) Analysis of Markovian jump stochastic Cohen-Grossberg bam neural networks with time delays for exponential input-to-state stability. Neural Process Lett 55(8):11055–11072. https://doi.org/10.1007/s11063-023-11364-4

Ravikanti DK, Saravanan S (2023) EEGAlzheimer'sNet: development of transformer-based attention long short term memory network for detecting Alzheimer disease using EEG signal. Biomed Signal Process Control 86:105318. https://doi.org/10.1016/j.bspc.2023.105318

Sadegh-Zadeh S-A, Fakhri E, Bahrami M, Bagheri E, Khamsehashari R, Noroozian M, Hajiyavand AM (2023) An approach toward artificial intelligence Alzheimer's disease diagnosis using brain signals. Diagnostics 13(3):477

Safi MS, Safi SMM (2021) Early detection of Alzheimer's disease from EEG signals using Hjorth parameters. Biomed Signal Process Control 65:102338. https://doi.org/10.1016/j.bspc.2020.102338

Siuly S, Alcin OF, Wang H, Li Y, Wen P (2024) Exploring rhythms and channels-based EEG biomarkers for early detection of Alzheimer's disease. IEEE Trans Emerg Top Comput Intell. https://doi.org/10.1109/TETCI.2024.3353610

Tharwat A (2021) Classification assessment methods. Appl Comput Inform 17:168–192. https://doi.org/10.1016/j.aci.2018.08.003

Wang W, Sun D (2021) The improved adaboost algorithms for imbalanced data classification. Inf Sci 563:358–374. https://doi.org/10.1016/j.ins.2021.03.042

Wang Z, Song J, Wang Y, Liu W (2023) Alzheimer's disease classification detection based on brain electrical signal graph structure. In: 2023 3rd international conference on frontiers of electronics, information and computation technologies (ICFEICT), pp 294–300. https://doi.org/10.1109/ICFEICT59519.2023.00057

Yuan S, Liu J-X, Shang J, Kong X, Ma Z (2018) The earth mover's distance and Bayesian linear discriminant analysis for epileptic seizure detection in scalp EEG. Biomed Eng Lett. https://doi.org/10.1007/s13534-018-0082-3

Zheng X, Wang B, Liu H, Wu W, Sun J, Fang W, Jiang R, Hu Y, Jin C, Wei X et al (2023) Diagnosis of Alzheimer's disease via resting-state EEG: integration of spectrum, complexity, and synchronization signal features. Front Aging Neurosci 15